ELSEVIER

11 December 2000

PHYSICS LETTERS A

Physics Letters A 277 (2000) 345–351

www.elsevier.nl/locate/pla

Numerical studies on bi-directionally coupled directly modulated semiconductor lasers

V. Bindu, V.M. Nandakumaran *

International School of Photonics, Cochin University of Science and Technology, Cochin 682 022, Kerala, India

Received 3 December 1999; received in revised form 5 July 2000; accepted 22 September 2000
Communicated by A.R. Bishop

Abstract

Results of a numerical study of synchronisation of two directly modulated semiconductor lasers, using bi-directional coupling, are presented. The effect of stepwise increase in the coupling strength (C) on the synchronisation of the chaotic outputs of two such lasers is studied, with the help of parameter space plots, synchronisation error plots, phase diagrams and time series outputs. Numerical results indicate that as C increases, the system achieves synchronisation as well as stability together with an increase in the output power. The stability of the synchronised states is checked by applying a perturbation to the system after it becomes synchronised and then noting the time it takes to regain synchronisation. For lower values of C the system does not regain synchronisation. But, with higher values synchronisation is regained within a very short time.

PACS: 05.45; 42.50; 42.55.b
Keywords: Synchronisation; Bi-directional coupling; Directly modulated semiconductor lasers

1. Introduction

Chaotic synchronisation is one of the extensively studied areas of research, in the last few years [1–7] because of its potential applications in the field of private communication [8–13]. Synchronisation can also be effectively employed for the control of chaos in different dynamical systems [14–19]. Different methods like occasional coupling [20], uni-directional coupling [21,22], etc. have been recently shown to induce synchronisation between chaotic systems. Feedback methods are also widely used for synchronisation purposes [23,24]. Synchronisation of various lasers have been achieved in various studies recently [25–28].

A method of bi-directional coupling has been recently used to stabilise or control the chaotic outputs of directly modulated semiconductor lasers [29]. This scheme is used here for synchronising the outputs of two such lasers starting from two different initial conditions. Such lasers have several practical applications in high capacity information transmission, ultrafast optical processing and high-speed pulse generation [29]. Since InGaAsP lasers are widely used in optical communication systems, synchronisation of two such lasers will be of practical value. Theoretically, it has been shown that the present system exhibits chaos for certain range of parameter values. This has been validated experimentally as well [30–32]. Several investigators [33–35] have studied the effect of the

* Corresponding author.
E-mail address: photonix@vsnl.com (V.M. Nandakumaran).

0375-9601/00/$ – see front matter
PII: S0375-9601(00)00637-X

spontaneous emission factor, Auger combination factor and the nonlinear gain reduction factor. Suppression of chaos in the output of such lasers has been achieved by two different methods in [29] and [35]. The present study shows that two such lasers can be synchronised and at the same time can be brought to stability together with an increase in the output amplitude. The Letter is organised as follows. Section 2 contains a general formulation of the method of bidirectional coupling. Section 3 presents the results of the numerical study of the dynamics of the coupled system. The last section contains our conclusions.

2. Laser model

Semiconductor lasers with direct current modulation can be well represented by the following rate equations governing the photon density (P), carrier density (N), and driving current (I) [35]:

$$\frac{dN}{dt} = \frac{1}{\tau_e}\left\{\left(\frac{I}{I_{th}}\right) - N - \left[\frac{N-\delta}{1-\delta}\right]P\right\}, \tag{1}$$

$$\frac{dP}{dt} = \frac{1}{\tau_p}\left\{\left[\frac{N-\delta}{1-\delta}\right](1-\varepsilon P)P - P + \beta N\right\}, \tag{2}$$

$$I(t) = I_b + I_m \sin(2\pi f_m t), \tag{3}$$

where τ_e and τ_p are the electron and photon lifetimes, N and P are the carrier and photon densities, I is the driving current, $\delta = n_0/n_{th}$, $\varepsilon = \varepsilon_{NL} S_0$ are dimensionless parameters where n_0 is the carrier density required for transparency, $n_{th} = (\tau_e I_{th}/eV)$ is the threshold carrier density, ε_{NL} is the factor governing the nonlinear gain reduction occurring with an increase in S, $S_0 = \Gamma(\tau_p/\tau_e)n_{th}$, I_{th} is the threshold current, e is the electron charge, V is the active volume and Γ is the confinement factor. I_b is the bias current, I_m is the amplitude of the modulation current, f_m is the modulation frequency and β is the spontaneous emission factor. Coupling is done by adding a current proportional to the output power of the first laser to the input of the second and vice versa. Initially the two lasers are set to operate at slightly different regions of the phase space. The rate equations governing the processes are [29]

$$\frac{dN_1}{dt} = \frac{1}{\tau_e}\left\{\left(\frac{I_1}{I_{th}}\right) - N_1 - \left[\frac{N_1-\delta}{1-\delta}\right]P_1\right\}, \tag{4}$$

$$\frac{dP_1}{dt} = \frac{1}{\tau_p}\left\{\left[\frac{N_1-\delta}{1-\delta}\right](1-\varepsilon P_1)P_1 - P_1 + \beta N_1\right\}, \tag{5}$$

$$I_1(t) = I_b + I_m \sin(2\pi f_m t) + C P_2, \tag{6}$$

$$\frac{dN_2}{dt} = \frac{1}{\tau_e}\left\{\left(\frac{I_2}{I_{th}}\right) - N_2 - \left[\frac{N_2-\delta}{1-\delta}\right]P_2\right\}, \tag{7}$$

$$\frac{dP_2}{dt} = \frac{1}{\tau_p}\left\{\left[\frac{N_2-\delta}{1-\delta}\right](1-\varepsilon P_2)P_2 - P_2 + \beta N_2\right\}, \tag{8}$$

$$I_2(t) = I_b + I_m \sin(2\pi f_m t) + C P_1, \tag{9}$$

where C is the coupling strength. N_1 and P_1 refer to the carrier and photon densities of laser 1 and N_2 and P_2 to the same quantities of laser 2. The parameter values are so chosen that they match with those for InGaAsP, and also in the range where the outputs will be chaotic. The parameter values are as used in [35], so that the outputs will be chaotic without coupling.

3. Results and discussion

The rate equations (4)–(9) are solved numerically using the fourth-order Runge–Kutta method with step size in the picosecond range. The parameter space plots P_1 vs. P_2 are drawn for each value of the coupling strength C. The use of a parameter space plot for checking the synchronisation has been used earlier [36]. The parameter space plot shows no synchronisation between the two outputs for low values of coupling strength such as $C = 1$ and 2. From $C = 3$ onwards, the outputs P_1 and P_2 get synchronised (Figs. 1(a) and (b)). For a confirmation of the above points, the synchronisation error between the outputs P_1 and P_2 (i.e., error $= |P_1 - P_2|$) is calculated and plotted against the corresponding time. These graphs can be used for finding out the synchronisation times also. For low values of C the initial error increases to very high values and remains high even in the long run. This indicates lack of synchronisation between P_1 and P_2. As C increases, the error, even though initially grows to slightly high values, soon decays off to zero within a few nanoseconds. The decay of error becomes faster with an increase in the coupling strength. These are evident from Figs. 2(a) and (b).

The time series of the outputs of the two lasers for different C values are shown in Figs. 3(a) and (b).

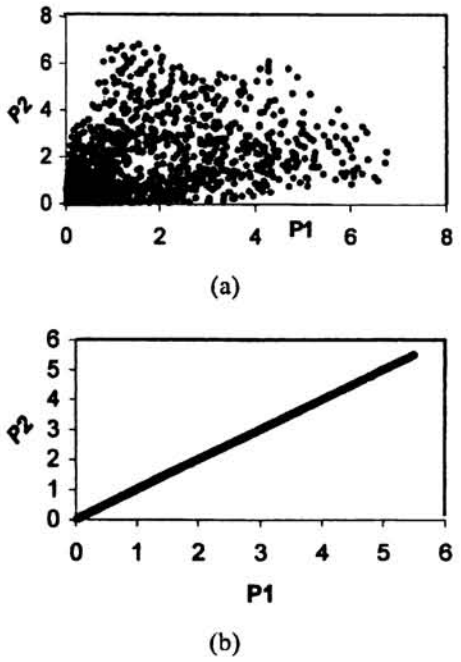

Fig. 1. (a) Photon density of laser 1 (P_1) vs. photon density of laser 2 (P_2) for coupling strength $C = 2$. (b) Photon density of laser 1 (P_1) vs. photon density of laser 2 (P_2) for coupling strength $C = 3$.

For coupling values from 1 to 17, the time series of P_1 and P_2 shows a double peak structure. For C values above 18 this second peak inside a single modulation period almost disappears, simultaneously with an increase in the output power. Figs. 3(a) and (b) show the time series of the output P_2 at $C = 2$ and $C = 20$, respectively. For C values from 18 to 25 the suppression of double peak which is associated with a deformation of the phase plot becomes more pronounced. The phase diagrams show that the system, after achieving synchronisation at $C = 3$, undergoes a reverse period doubling with a four cycle at $C = 6$; a period two cycle at $C = 9$; and a period one cycle at $C = 17$ (Figs. 4(a)–(d)). With further increase of C, the phase diagrams start getting deformed and with $C = 26$, the phase diagrams becomes a single closed curve without the notch that was present for small values of C (Fig. 4(e)). This confirms the suppression of the double peak structure.

A reverse period doubling route to stability and a suppression of the double peak, and a high increase in the output power are apparent here. Above all, there

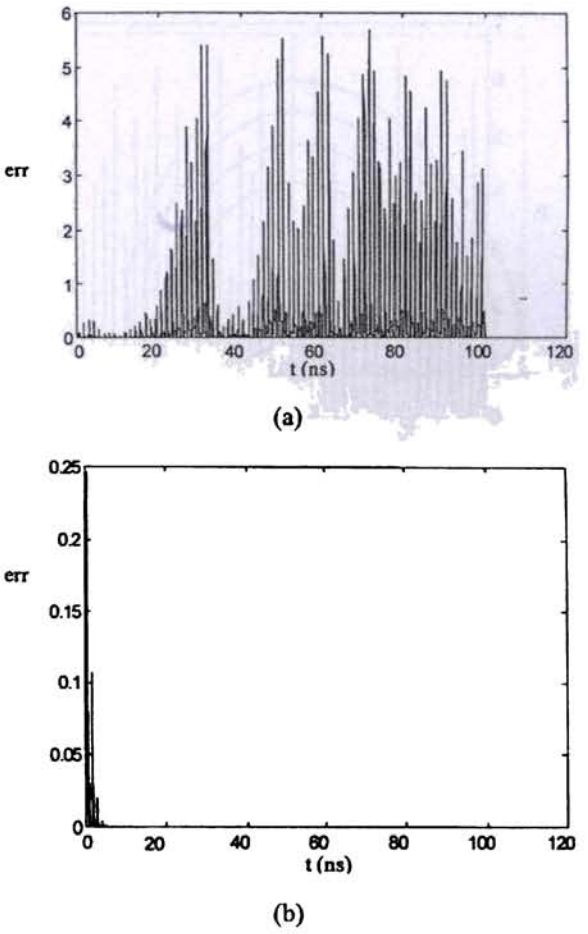

Fig. 2. (a) Error (err) vs. corresponding time (t) without perturbation for coupling strength $C = 2$. (b) Error (err) vs. corresponding time (t) without perturbation for coupling strength $C = 20$.

is synchronisation between the two outputs at all these stages of the system dynamics. It is due to the terms CP_1 and CP_2 in Eqs. (6) and (9) that synchronisation, reverse period doubling and suppression of the second peak are achieved. All these and an increase in the output power are obtained by giving a bi-directional coupling between the two lasers.

The double peak within a single modulation period has been explained as a manifestation of relaxation oscillation which gets damped by an increase in ε, the term governing nonlinear gain reduction, which also eliminates the period doubling as well [35]. There, the double peak structure and period doubling were suppressed by an increase in ε, but at the cost of

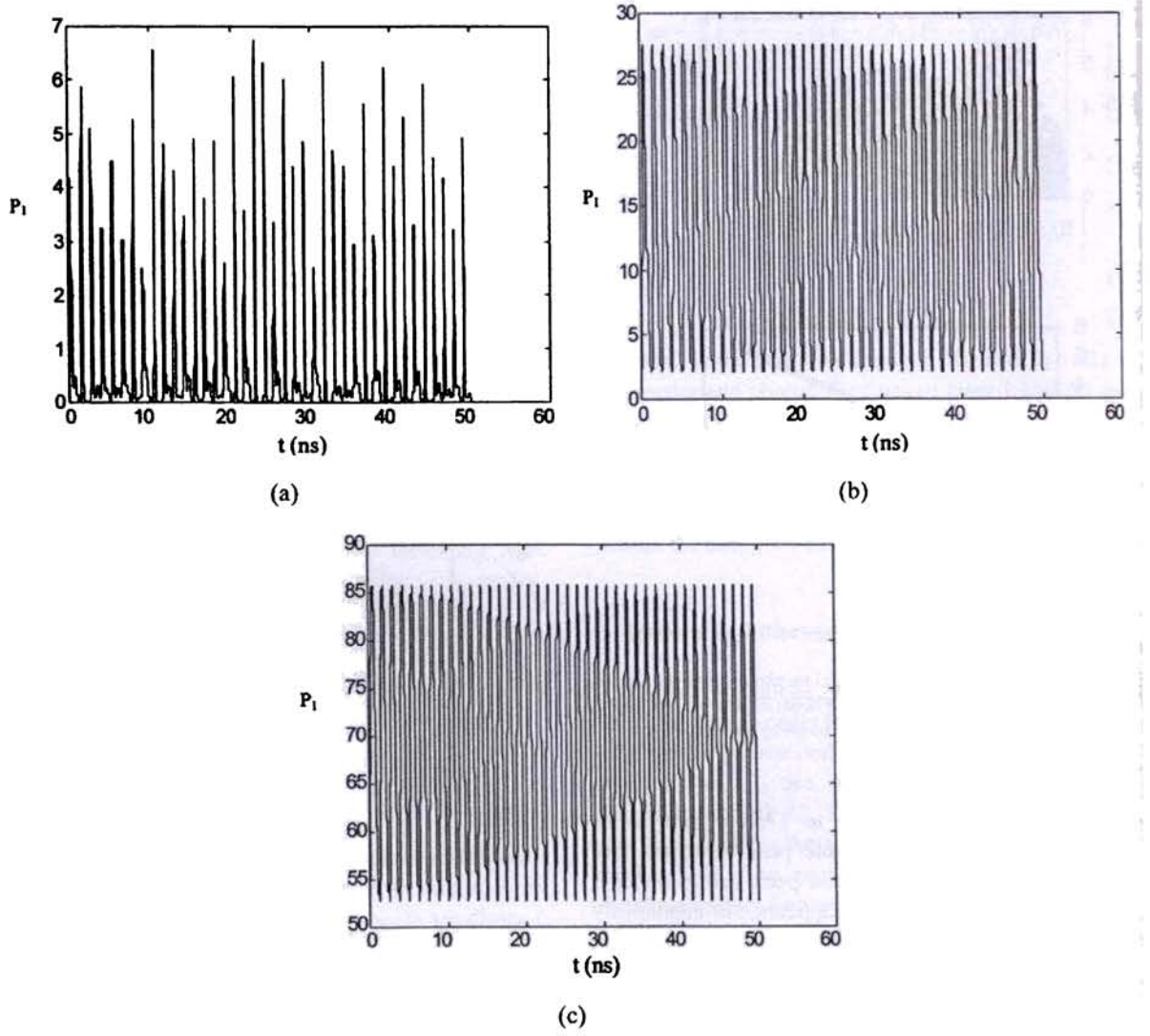

Fig. 3. (a) Time series of photon density of laser 1 (P_1) for coupling strength $C = 2$. (b) Time series of photon density of laser 2 (P_2) for coupling strength $C = 20$. (c) Time series of photon density of laser 1 (P_1) for coupling strength $C = 26$.

the output power. But, the present results show a definite advantage as it provides an alternate method for suppressing the second peak together with an increase in the output power. The time series of output P_2 at $C = 26$ given in Fig. 3(c) shows the increase in the output power.

To check the stability of the synchronised state, we perturb the system. After eliminating the transients, when the error becomes small so that the system can be considered in synchronisation, P_1 and P_2 are externally changed. The error $|P_1 - P_2|$ is made as large as it was in the beginning. This is done for each value of coupling strength and the corresponding error plots are taken. Since for C values less than 3, the system never achieves synchronisation, artificial perturbation is not applied in this range. From $C = 3$ onwards, perturbation is applied when the two outputs are in synchronisation. The corresponding error plots

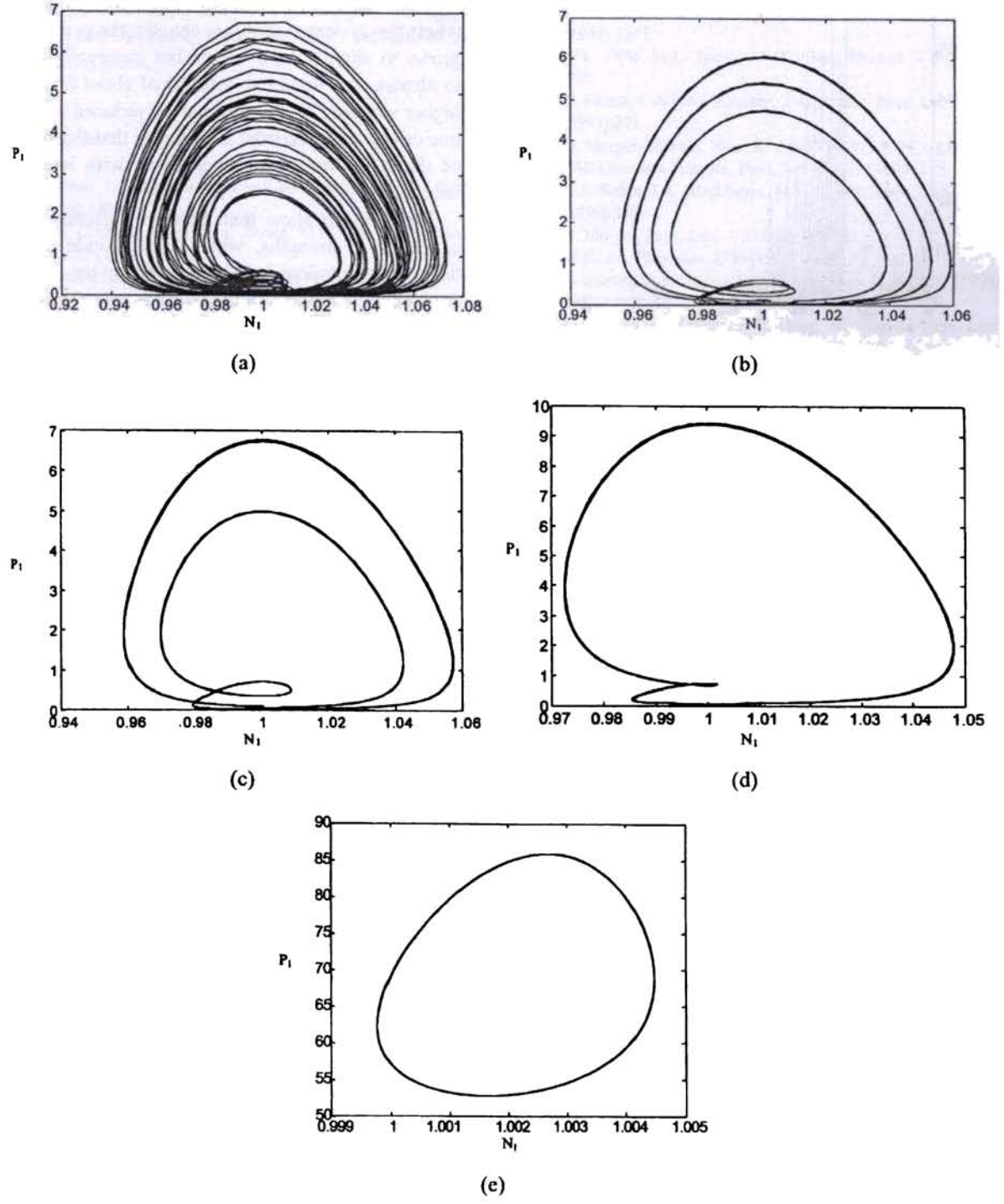

Fig. 4. (a) Phase plots (photon density along x axis and carrier density along y axis) of laser 1 and laser 2 for coupling strength (a) $C = 3$, (b) $C = 6$, (c) $C = 9$, (d) $C = 17$, (e) $C = 26$.

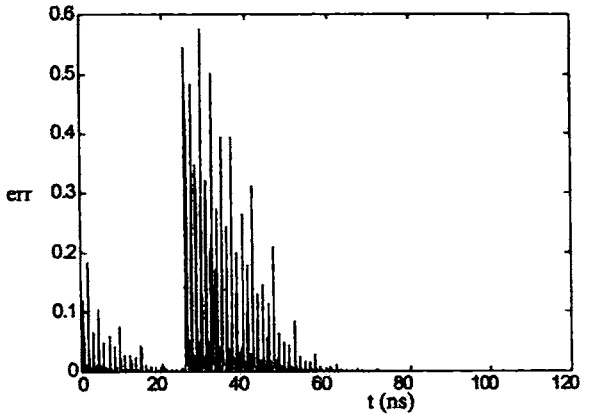

(a)

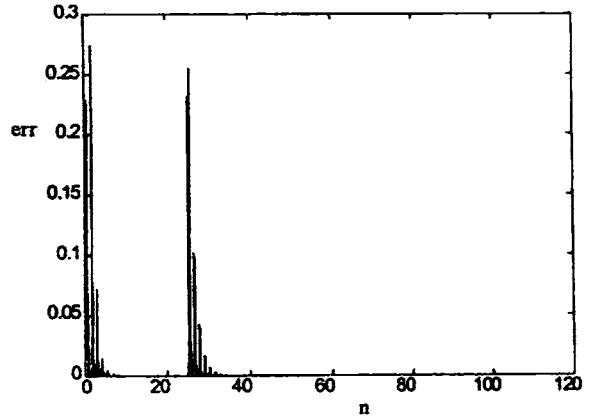

(b)

Fig. 5. (a) Error (err) vs. corresponding time (t) with perturbation for coupling strength $C = 6$. (b) Error (err) vs. corresponding time (t) with perturbation for coupling strength $C = 20$.

are shown in Figs. 5(a) and (b). For small values of C, where the system outputs are chaotic, the perturbation grows to slightly high values but eventually decays to almost zero within an interval of about 20 ns. For higher values of C, this interval get reduced to around one or two nanoseconds. This shows that the stability of the synchronised states increase with increasing values of C.

These results show that there are different ranges of coupling strengths, which can provide us with different dynamical behaviours. Thus, by choosing appropriate coupling values, we can use the method of bi-directional coupling for chaotic synchronisation, suppression of chaos, or for high gain outputs.

Table 1 shows the different coupling values and the corresponding dynamics of the systems.

4. Conclusion

The above studies show that by the method of bi-directional coupling, we can suppress chaos and the double peak, and have synchronisation between the two outputs together with a high increase in the output power. The bi-directional coupling scheme brings forth a variety of dynamical behaviour from the system and is therefore a very interesting system for further investigations.

Acknowledgement

V.B. wishes to thank CUSAT, Cochin for financial assistance through a junior research fellowship, and

Table 1
Coupling strengths and the corresponding dynamics

Coupling strength, C	Dynamics	Synchronisation	Max. amp
1, 2	Chaotic	No	6 units
3 to 5	Chaotic	Yes	6 units
6	Four cycle	Yes	6 units
7, 8	Four cycle	Yes	>6 <8 units
9 to 16	Two cycle	Yes	>7 <10 units
17 to 25	One cycle	Yes	>10 <30 units
26	One cycle	Yes	~85

V.M.N. acknowledges the financial support through a minor research project under the UGC scheme of an unassigned grant.

References

[1] S. Kaart, J.C. Schoten, C.M. van den Bleek, Phys. Rev. E 59 (1999) 5303.
[2] L.O. Chua, T. Yang, G.-q. Zhong, C.W. Wu, IEEE Trans. CAS 43 (1996) 862.
[3] P. Celka, IEEE Trans. CAS 43 (1996) 869.
[4] A.L. Fradkov, A.Y. Markov, IEEE Trans. CAS 44 (1997) 905.
[5] R. Roy, T.W. Murphy, T.D. Maier, Z. Gills, E.R. Hunt, Phys. Rev. Lett. 68 (1992) 1259.
[6] T.L. Carroll, G.A. Johnson, Phys. Rev. E 57 (1998) 1555.
[7] M.G. Rosenblum, A.S. Pikovsky, J. Kurths, Phys. Rev. Lett. 78 (1997) 4193.
[8] O. Morgul, M. Feki, Phys. Lett. A 251 (1999) 169.
[9] M.J. Bunner, W. Just, Phys. Rev. E 58 (1998) R4072.
[10] L.M. Pecora, T.L. Carroll, G. Johnson, D. Mar, Phys. Rev. E 56 (1997) 5090.
[11] P. Colet, R. Roy, Opt. Lett. 19 (1994) 2056.
[12] G. van Wiggeren, R. Roy, Science 279 (1998) 1198.
[13] A. Hohl, A. Gavrielides, T. Erneux, V. Kovanis, Phys. Rev. Lett. 78 (1997) 4745.
[14] K. Pyragas, Phys. Lett. A 170 (1992) 421.
[15] N.F. Rulkov, L.S. Tsimring, H.D.I. Abarbanel, Phys. Rev. E 50 (1994) 314.
[16] R. Femat, J. Alvarez-Ramirez, IEEE Trans. CAS 46 (1999) 1150.
[17] J.E.S. Socolar, D.W. Sukow, D.J. Gauthier, Phys. Rev. E 50 (1994) 3245.
[18] W.L. Ditto, M.L. Spano, J.F. Lindner, Physica D 86 (1995) 198.
[19] R. Femat, J. Alvarez-Ramirez, J. Gonzalez, Phys. Lett. A 224 (1997) 271.
[20] O. Morgul, M. Feki, Phys. Rev. E 55 (1997) 5004.
[21] J.M. Gonzales-Miranda, Phys. Lett. A 251 (1999) 115.
[22] G.L. Baker, J.A. Blackbuyrn, H.J.T. Smith, Phys. Lett. A 252 (1999) 191.
[23] O. Morgul, Phys. Lett. A 247 (1998) 391.
[24] M.K. Ali, Phys. Rev. E 55 (1997) 4804.
[25] G. Santobini, A. Varone, S.R. Bishop, Phys. Lett. A 257 (1999) 175.
[26] L. Yawowen, L.I. Haiben, Z. Hong, W. Yinghai, Phys. Lett. A 256 (1999) 166.
[27] D.Y. Tang, R. Dykstra, M.W. Hamilton, N.R. Heckenbeg, Phys. Rev. E 57 (1998) 5247.
[28] R. Roy, K.S. Thornburg Jr., Phys. Rev. Lett 72 (1994) 3501.
[29] T. Kuruvilla, V.M. Nandakumaran, Phys. Lett. A 254 (1999) 59.
[30] H.G. Winful, Y.C. Chen, J.M. Lin, Appl. Phys. Lett. 48 (1986) 161.
[31] M. Tang, S. Wang, Appl. Phys. Lett. 48 (1986) 900.
[32] Y. Hori, H. Serisava, H. Sato, J. Opt. Soc. Am. B 5 (1988) 1128.
[33] H. Tang, S. Wang, Appl. Phys. Lett. 47 (1985) 208.
[34] H. Tang, S. Wang, Appl. Phys. Lett. 50 (1987) 1861.
[35] G.P. Agarwal, Appl. Phys. Lett. 49 (1986) 1013.
[36] P. Ashwin, J. Buescu, I. Stewart, Phys. Lett. A 193 (1994) 126.